STRUCTURAL BIOLOGY

Volume 73 (2017)

Supporting information for article:

Structural features of NS3 of *Dengue virus* serotypes 2 and 4 in solution and insight into the inhibitory role of quercetin and RNA binding

Ankita Pan, Wuan Geok Saw, Malathy Sony Subramanian Manimekalai, Ardina Grüber, Shin Joon, Tsutomu Matsui, Thomas M. Weiss and Gerhard Grüber

Supplementary Table S1: Extinction coefficients and molecular weights of proteins from DENV used in determination of protein concentration.

Protein samples	Extinction coefficient (M^{-1} cm^{-1})	Molecular weight (kDa)
DENV-4 NS2B$_{18}$NS3	103735	72
DENV-2 NS2B$_{18}$NS3	106590	71.4
DENV-2 NS2B$_{18}$NS3 mutant $_{174}$PPAVP$_{179}$	106590	71.8
DENV-2 Protease	41940	21.8
DENV-2 Helicase	64400	51.4

Supplementary Figure legends

Supplementary Figure S1: Purification of DENV-2 NS3 and its domains. The elution diagrams of (*A*) DENV-2 NS2B$_{18}$NS3 using Superdex™ 200 HR 10/300 column as well as the (*B*) DENV-2 NS2B$_{18}$-protease and (*C*) -helicase using Superdex™ 75 HR 10/300 column. The fractions of the shaded region were pooled and concentrated for SAXS studies. (*Inset*) SDS-gel (17%) of the purified (*A*) DENV-2 NS2B$_{18}$NS3, (*B*) NS2B$_{18}$-Protease and (*C*) helicase, together with protein marker in *lane 1*.

Supplementary Figure S2: Concentration dependency analysis of (*A*) DENV-4 NS2B$_{18}$NS3, (*B*) DENV-2 NS2B$_{18}$NS3 (*C*) DENV-2 NS3 mutant $_{174}$PPAVP$_{179}$, (*D*) DENV-2 NS2B$_{18}$Protease and (*E*) DENV-2 helicase. For DENV-4 NS2B$_{18}$NS3 the R_g and *I(0) versus* protein concentration plots showed an increase in both parameters at the highest protein concentration (5.4 mg/ml), therefore the data of the first two concentrations were merged. All other protein samples showed no significant concentration dependency.

Supplementary Figure S3: Guinier plots with the residual plots (●, *red*) for each fit line (—, *red*). (*A*) The Guinier region selected for scattering patterns of DENV-4 NS2B$_{18}$NS3 at protein concentrations of (i) 1.5 (●, *wine*), (ii) 2.8 (●, *orange*) and (iii) 5.4 mg/ml (●, *violet*) with $q_{min}R_g$ and $q_{max}R_g$ range of 0.59-1.21, 0.60-1.25, and 0.70-1.30, respectively. (*B*) The Guinier region selected for scattering patterns of DENV-2 NS2B$_{18}$NS3 at protein concentrations of (i) 1.2 (●, *wine*), (ii) 3.3 (●, *orange*) and (iii) 5.4 mg/ml (●, *violet*), which have the $q_{min}R_g$ and $q_{max}R_g$ range of 0.58-1.28, 0.60-1.30, and 0.60-1.25, respectively. (*C*) The Guinier region selected for scattering patterns of DENV-2 NS3 mutant $_{174}$PPAVP$_{179}$ at protein concentrations of (i) 1.1 (●,

wine), (ii) 3.0 (●, *orange*) and (iii) 5.0 mg/ml (●, *violet*), and having $q_{min}R_g$ and $q_{max}R_g$ range of 0.73-1.29, 0.72-1.30, and 0.70-1.29, respectively. (*D*) The Guinier region selected for scattering patterns of DENV-2 $NS2B_{18}$Protease at protein concentrations of (i) 1.6 (●, *wine*), (ii) 3.0 (●, *violet*) and (iii) 4.7 mg/ml (●, *green*), with $q_{min}R_g$ and $q_{max}R_g$ range of 0.48-1.27, 0.48-1.27, and 0.44-1.30, respectively. (*E*) The Guinier region selected for scattering patterns of DENV-2 helicase at protein concentrations of (i) 2.5 (●, *orange*), (ii) 3.0 (●, *cyan*) and (iii) 5.0 mg/ml (●, *magenta*), and having $q_{min}R_g$ and $q_{max}R_g$ range of 0.57-1.28, 0.53-1.23, and 0.51-1.10, respectively. (*F*) The Guinier region selected for scattering patterns of DENV-2 $NS2B_{18}$NS3 in the (i) absence (●, *black*) or presence of (ii) ATP (●, *red*), (iii) ADP (●, *green*), (iv) AMPPNP (●, *magenta*) and (v) RNA (●, *blue*), which has the $q_{min}R_g$ and $q_{max}R_g$ range of 0.34-1.28, 0.43-1.28, 0.40-1.30, 0.57-1.28, and 0.43-1.29, respectively. The residuals of Guinier fit line are shown at the *bottom* of each Guinier plot. Few data points at lower *q* region are not included in the Guinier calculation due to the higher deviation observed for these data points in the residual distribution.

Supplementary Figure S4: The fit of the scattering profiles derived from the *P(r)* function (—, *red*) to the experimental data (●, *black*) for (*A*) DENV-4 $NS2B_{18}$NS3, (*B*) DENV-2 $NS2B_{18}$NS3, (*C*) DENV-2 NS3 mutant $_{174}$PPAVP$_{179}$, (*D*) DENV-2 $NS2B_{18}$Protease, and (*E*) DENV-2 helicase.

Supplementary Figure S5: 700 MHz ^{1}H-^{15}N-HSQC spectrum of DENV2 NS3 protease, recorded at 298K on a Bruker Avance spectrometer. Resolved peaks of NH-resonances, including tryptophan side chain, are indicated in the number. In total, 203 peaks were observed

for 206 NH-resonances (195 non-proline residues and 11 tryptophan side chains). The side chain NH_2-resonances of asparagine- and glutamine are connected by horizontal lines. The extension of the overlapped region is shown in a separated box.

Supplementary Figure S6: SAXS studies of individual DENV-2 NS2B$_{18}$NS3 domains. (*A, B*) SAXS pattern of the DENV-2 protease (○; *violet*) and -helicase (○; *orange*). (*inset of A and B*) Guinier plots show linearity for both proteins, indicating no aggregation in all concentrations used. Since no concentration dependency was observed, 3.0 and 2.5 mg/ml measurements were used as the final composite scattering curve for protease and helicase domain, respectively. The scattering profiles in Guinier plots are offset for clarity by applying arbitrary scale factors. *(C)* Pair-distance distribution function *P(r)* of DENV-2 protease (—; *violet*) and -helicase (—; *orange*). (*D*) Normalized Kratky plot of DENV-2 NS2B$_{18}$NS3 (●; *red*) compared to the protease (●; *violet*) and helicase (●; *orange*), as well as the compact globular lysozyme (●; *grey*) with a peak (---; *grey*), representing the theoretical peak and assuming an ideal Guinier region of a globular particle. The scattering pattern of all three proteins exhibits a similar shift where their bell-shaped profiles shifted toward right with respect to standard globular proteins, indicating less rigidity in all three proteins.

Supplementary Figure S7: Comparison of SAXS scattering profiles of DENV-2 NS2B$_{18}$NS3 collected using the home-source BRUKER NANOSTAR SAXS instrument (○; *red*) and the synchrotron source at SSRL (●; *green*).

Supplementary Figure S8: Solution X-ray scattering studies of DENV-2 NS2B$_{18}$NS3 in the absence or presence of substrates collected at two protein concentrations (1.13 and 4.5 mg/ml). Although the scattering curves of both concentrations are virtually similar, Porod volumes and MW estimation at the higher concentration were slightly larger; therefore, the two scattering profiles were merged to achieve higher resolution data. The increase of Porod volume and estimated MW may be due to a concentration effect or improved data quality from the higher concentration. Comparison of (*A*) SAXS scattering patterns (○) and (*B*) *P(r)* functions (—) between the empty DENV-2 NS2B$_{18}$NS3 (*black*) and in the presence of nucleotides (ATP (*red*), ADP (*green*) or AMPPNP (*magenta*). The scattering profiles are offset for clarity by applying arbitrary scale factors. (*C*) Normalized Kratky plot of DENV-2 NS2B$_{18}$NS3 in the absence (●; *black*) or presence of ATP (●; *red*), ADP (●; *green*) and AMPPNP (●; *magenta*), compared to the compact globular lysozyme (●; *grey*) with a peak (---; *grey*), representing the theoretical peak and assuming an ideal Guinier region of a globular particle. The scattering patterns of NS2B$_{18}$NS3 in the absence or presence of nucleotides exhibit similar profiles where their bell-shaped profiles shifted towards right with respect to standard globular proteins, indicating no flexibility change in the absence or presence of nucleotides.

Supplementary Figure S9: Scattering profiles of free RNA (*magenta*), empty form of DENV-2 NS2B$_{18}$NS3 (*black*), the sum of the two curves (RNA and empty form) (*red*) and the RNA-bound complex of DENV-2 NS2B$_{18}$NS3 (*blue*) for 4.5 mg/ml data in (*A*) log-scale and (*B*) linear-scale of *I(q)*. The sum of the free species of RNA and empty form (*red*) is not the same as the RNA-bound form (*blue*), supporting that the RNA-bound complex have formed.

(A)

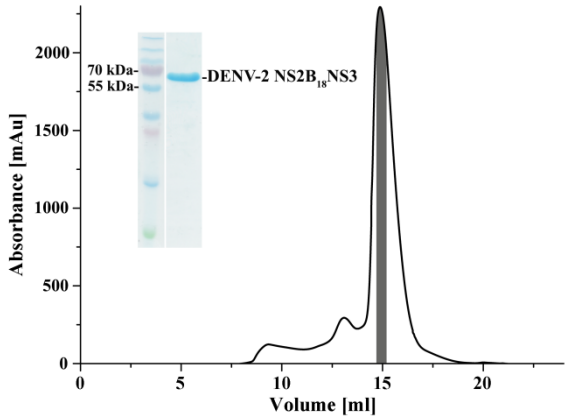

(B)

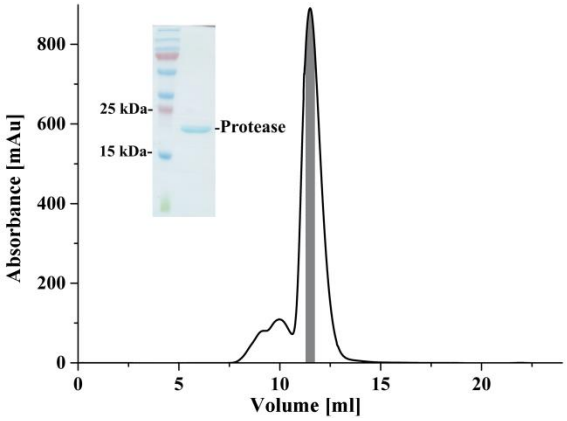

(C)

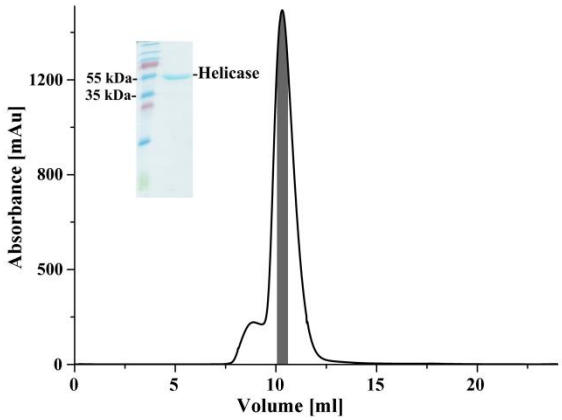

Supplementary Figures S1A-C

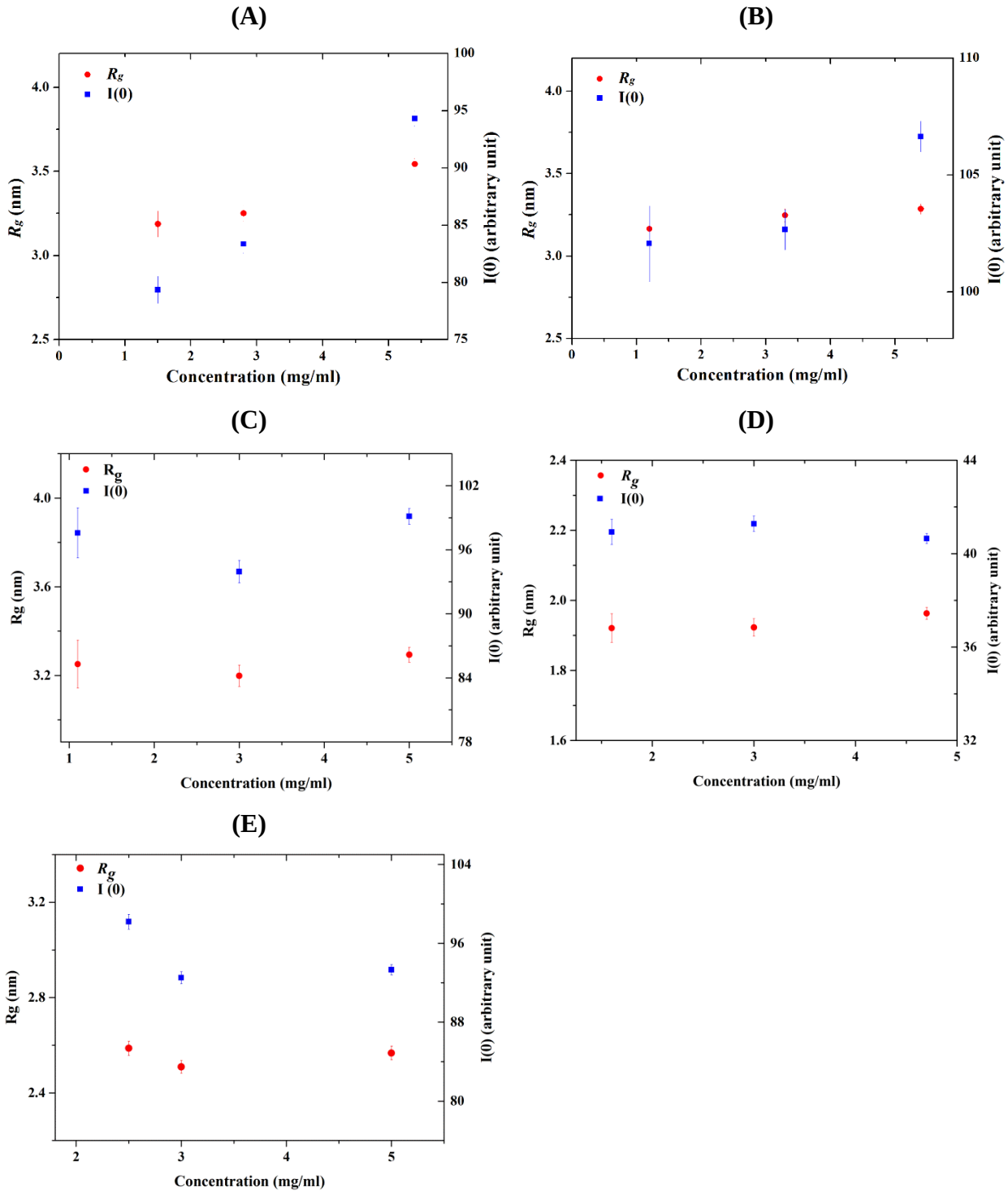

Supplementary Figures S2A-E

(A)

(i)

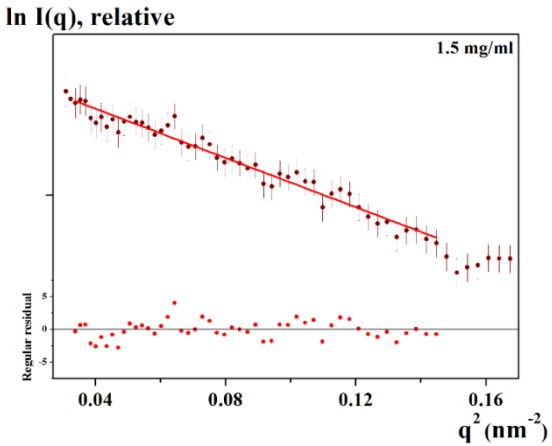

(ii)

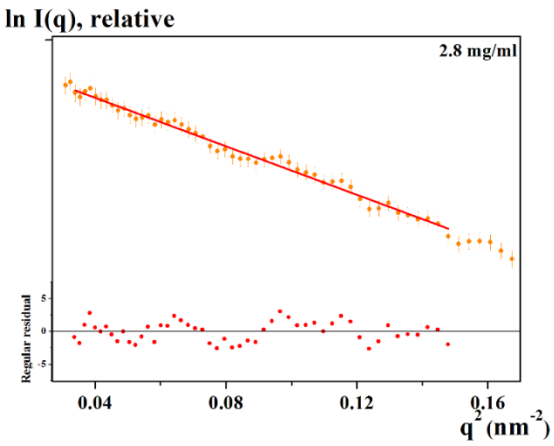

(iii)

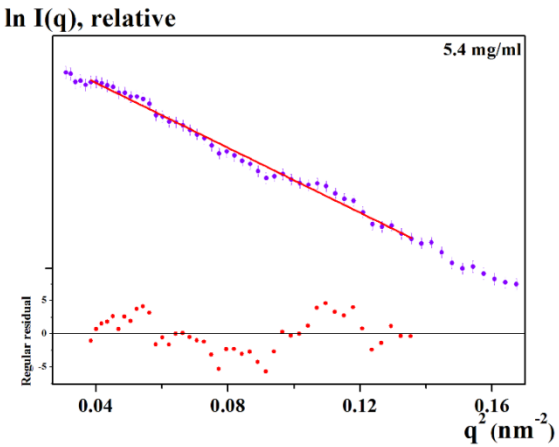

(B)

(i)

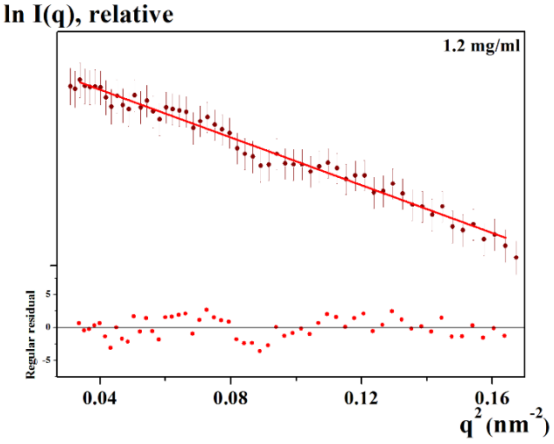

(ii)

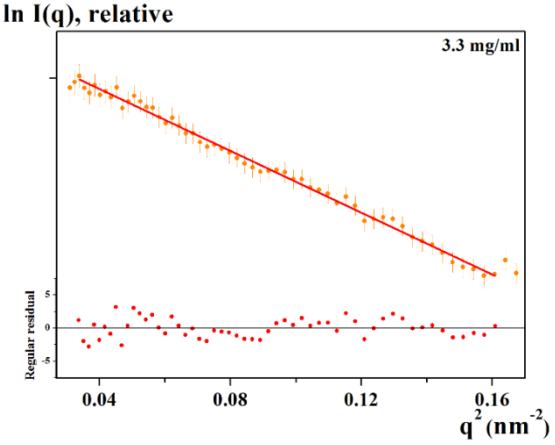

(iii)

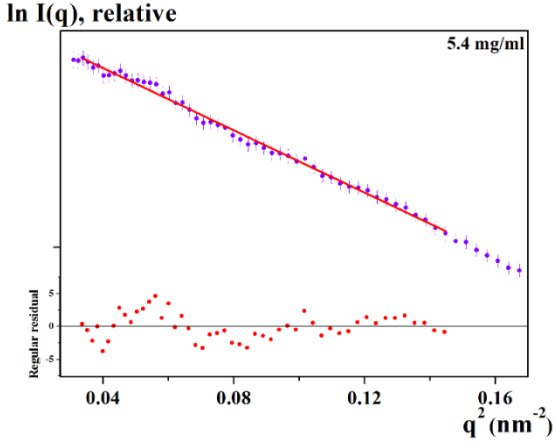

Supplementary Figures S3A-B

(C)

(i)

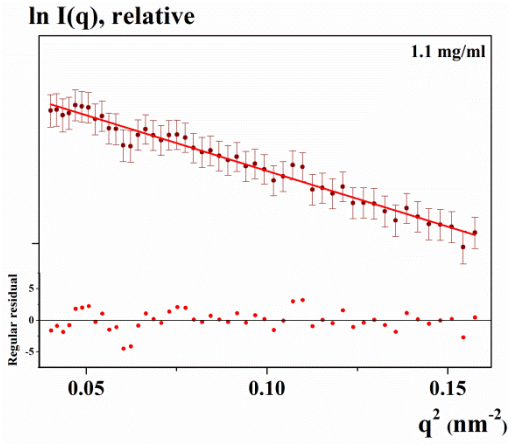

(ii)

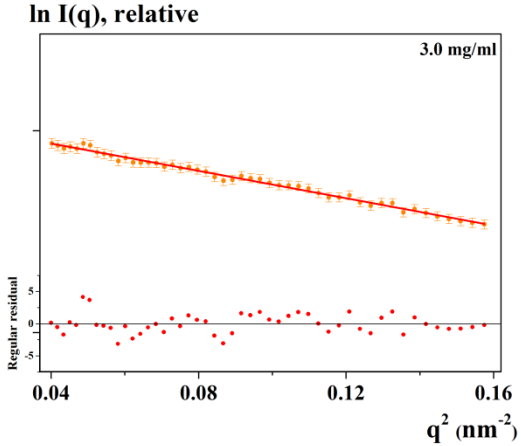

(iii)

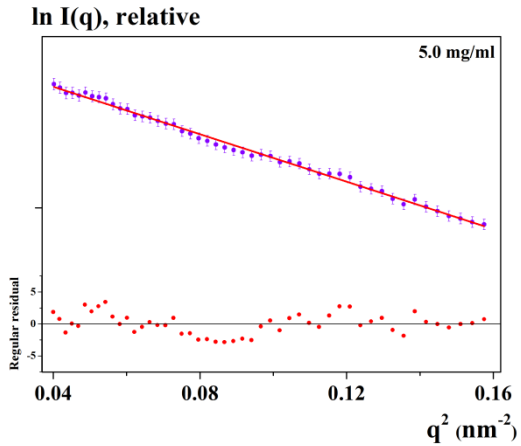

(D)

(i)

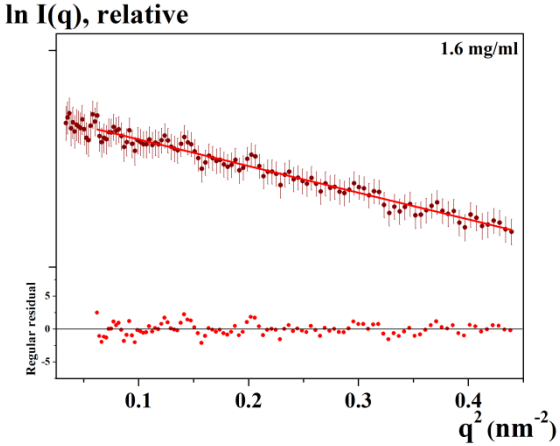

(ii)

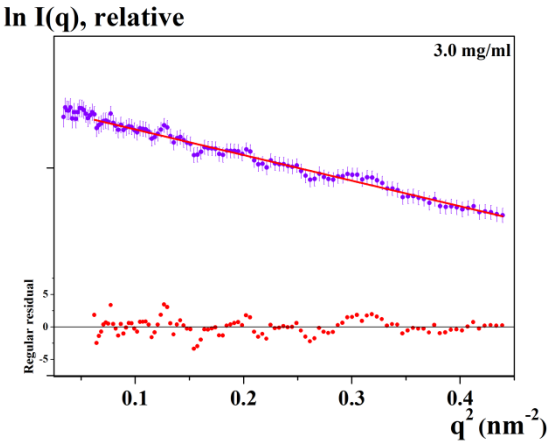

(iii)

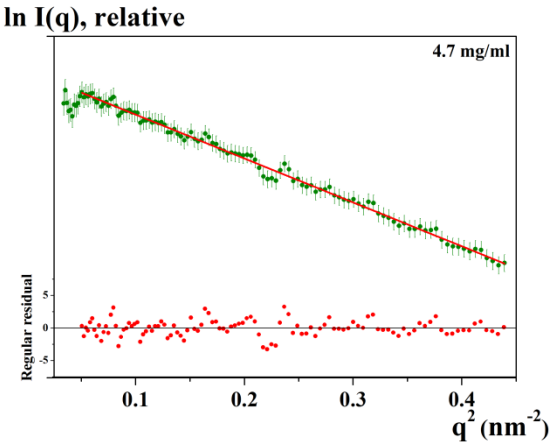

Supplementary Figures S3C-D

(E)

(i) **(ii)** **(iii)**

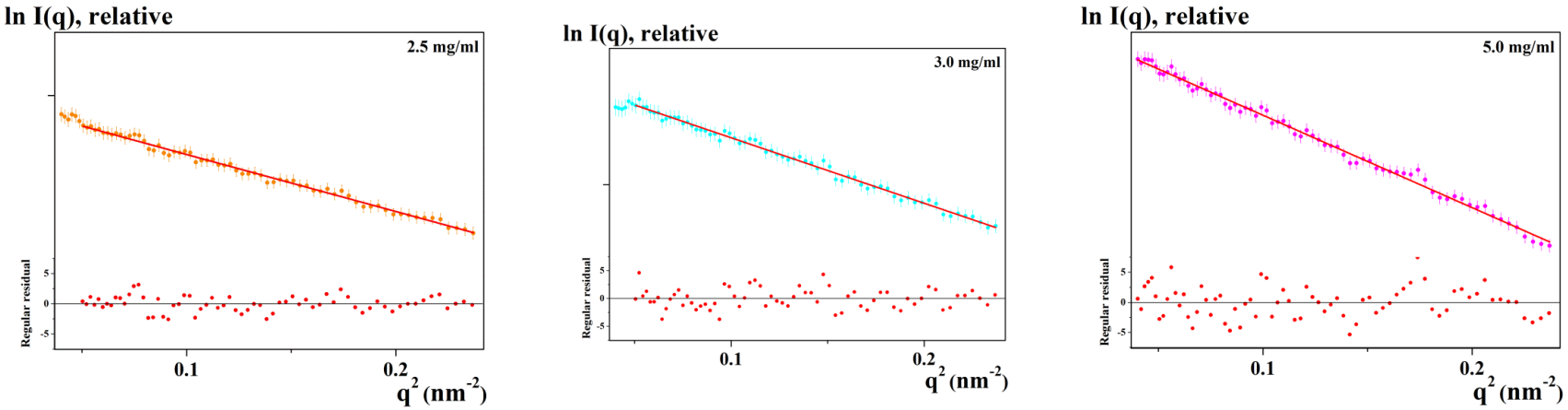

Supplementary Figures S3E

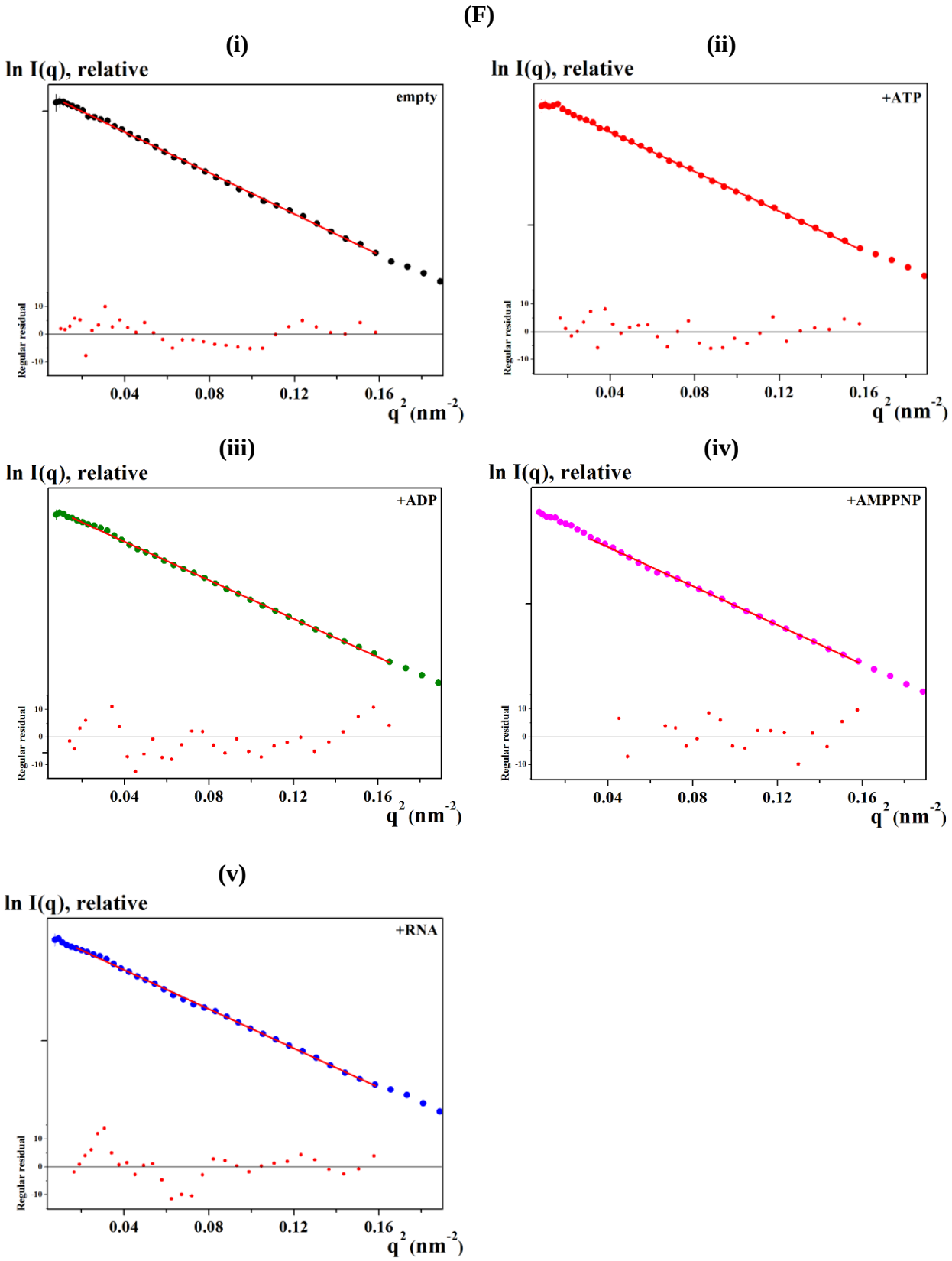

Supplementary Figure S3F

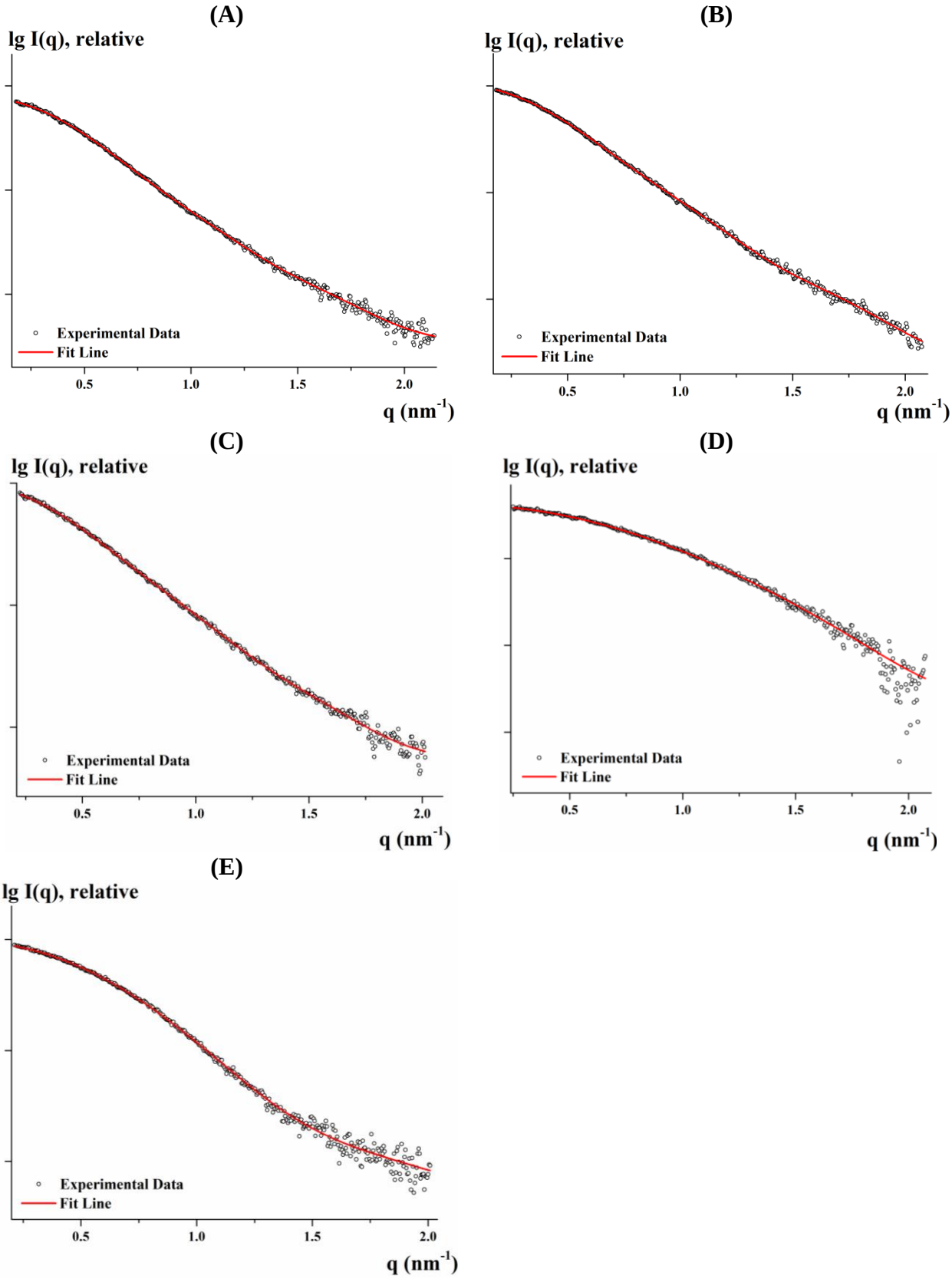

Supplementary Figures S4A-E

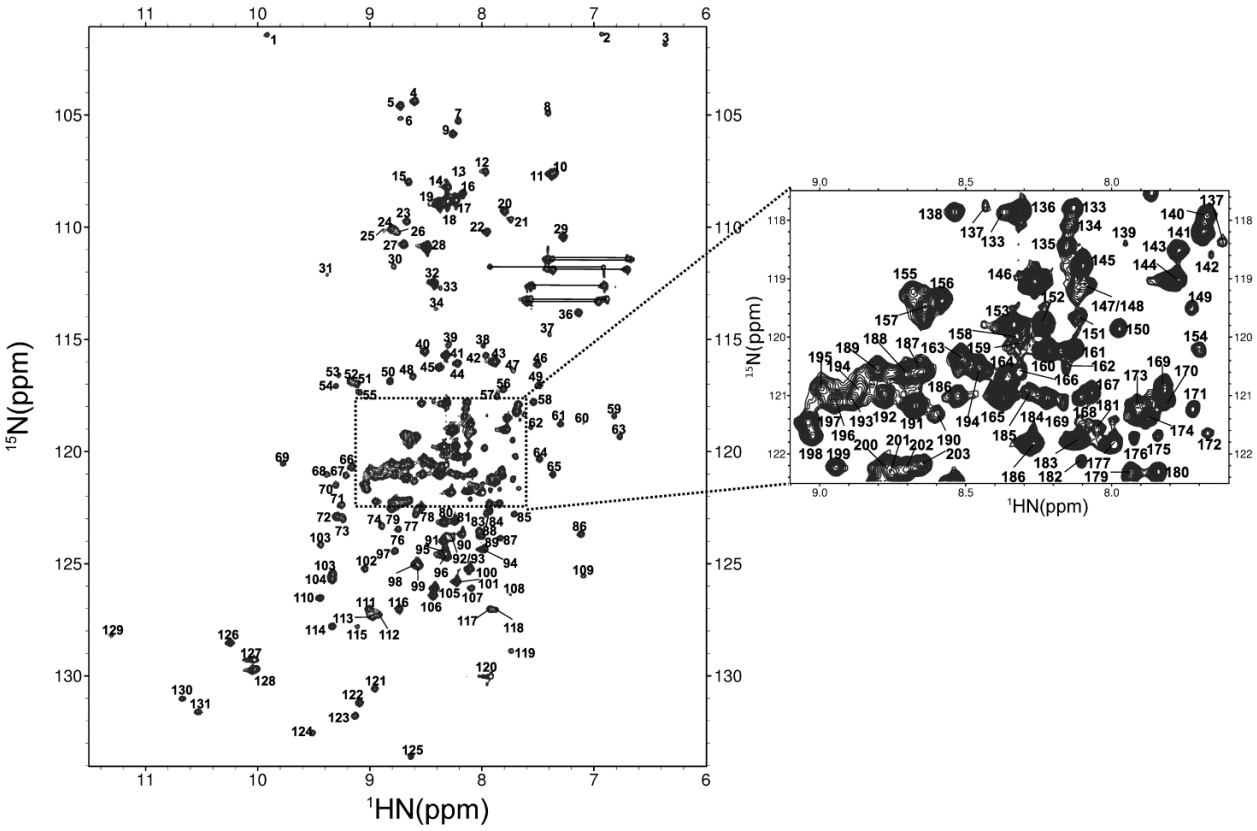

Supplementary Figure S5

(A) DENV-2 NS2B$_{18}$Protease

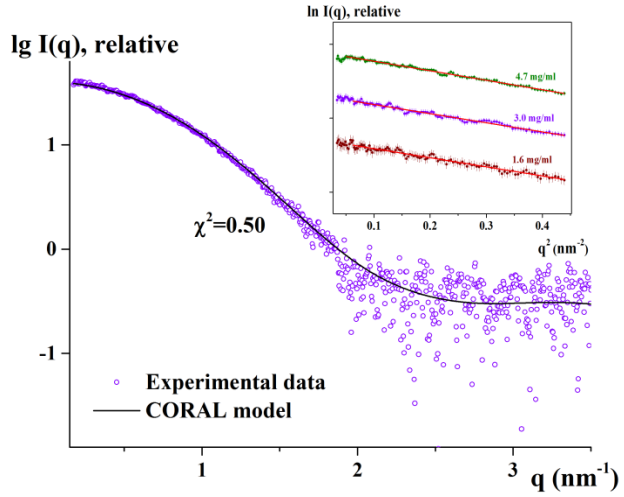

(B) DENV-2 Helicase

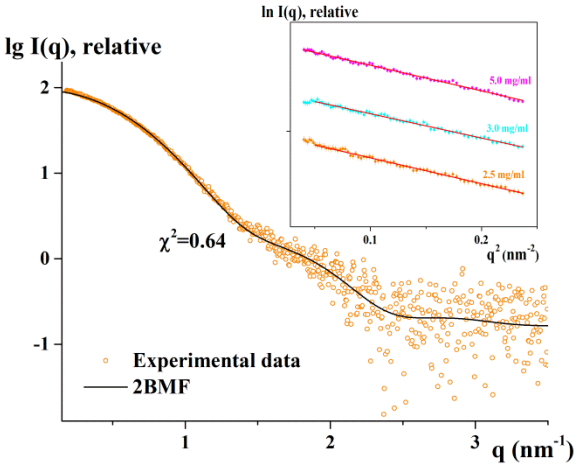

(C)

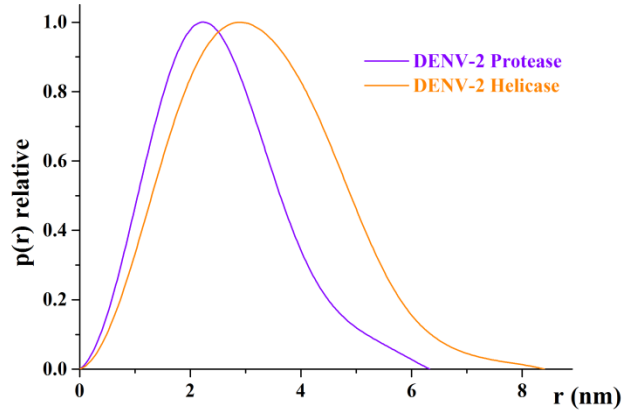

(D)

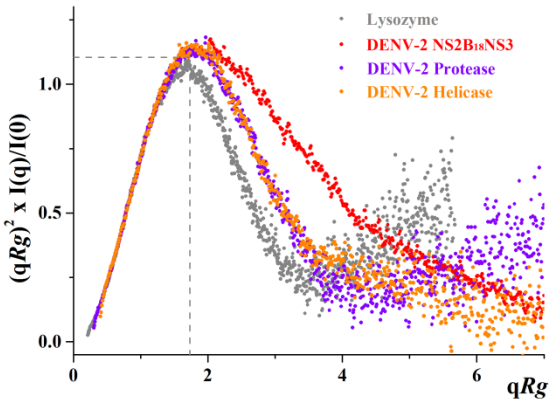

Supplementary Figure S6

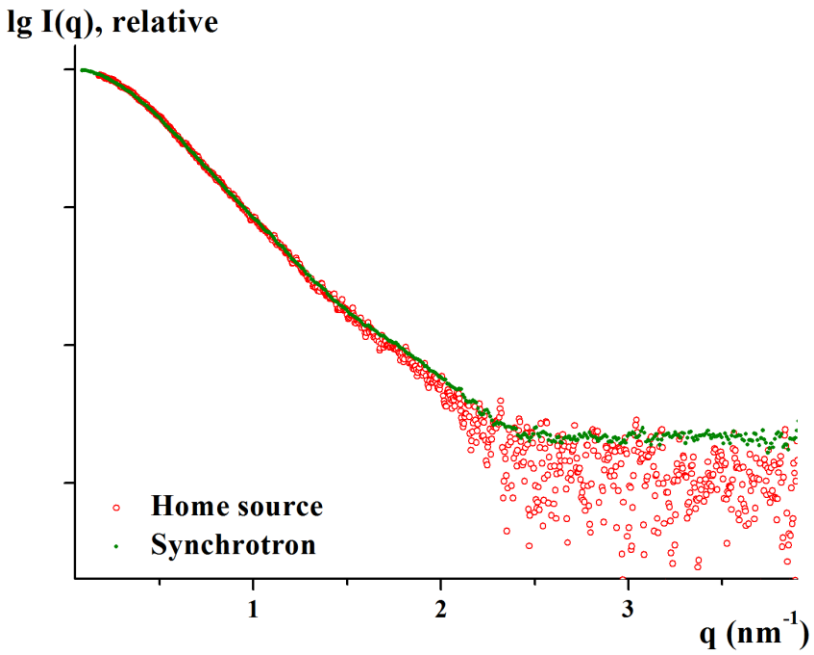

Supplementary Figure S7

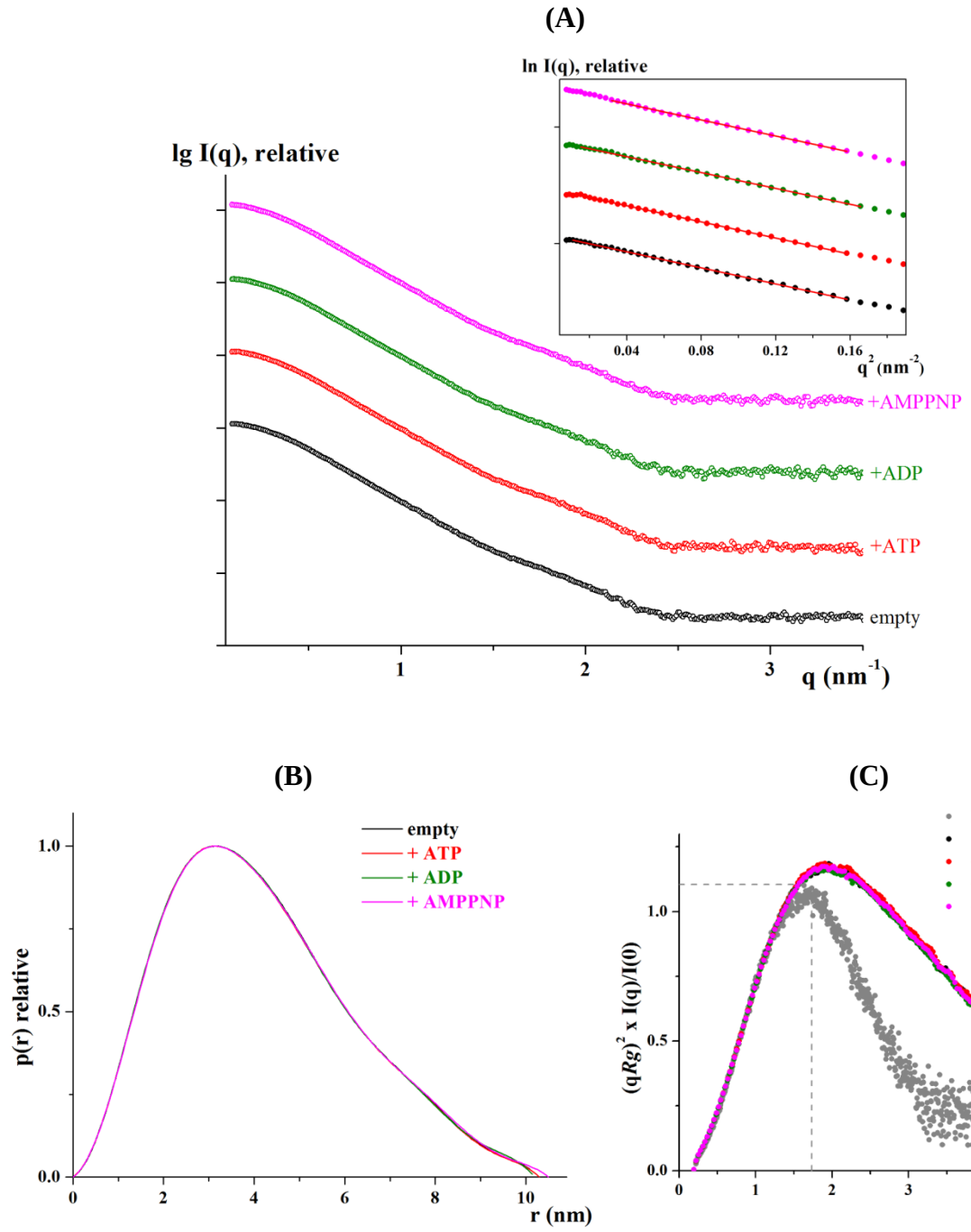

Supplementary Figure S8

(A)

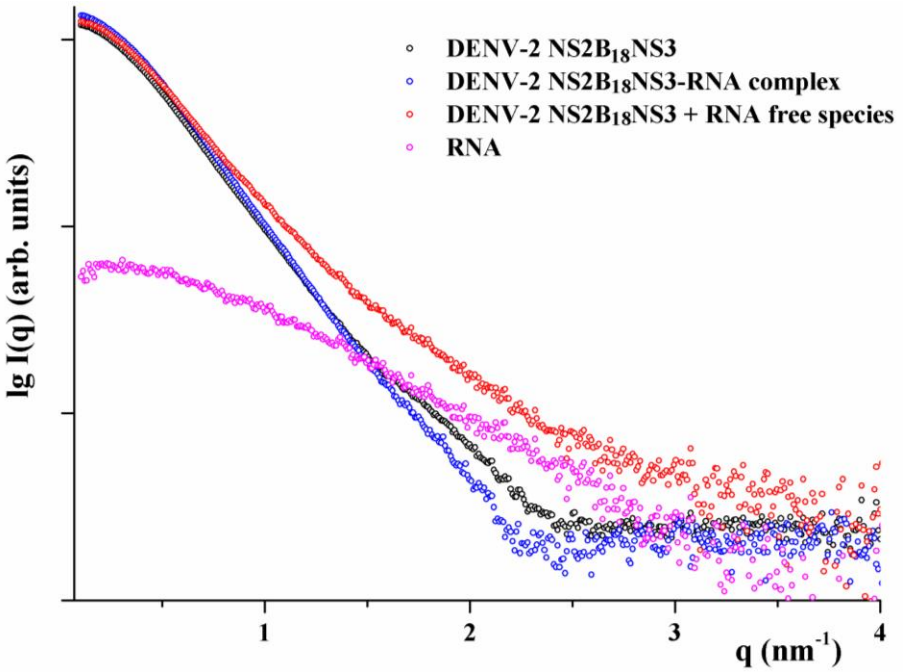

(B)

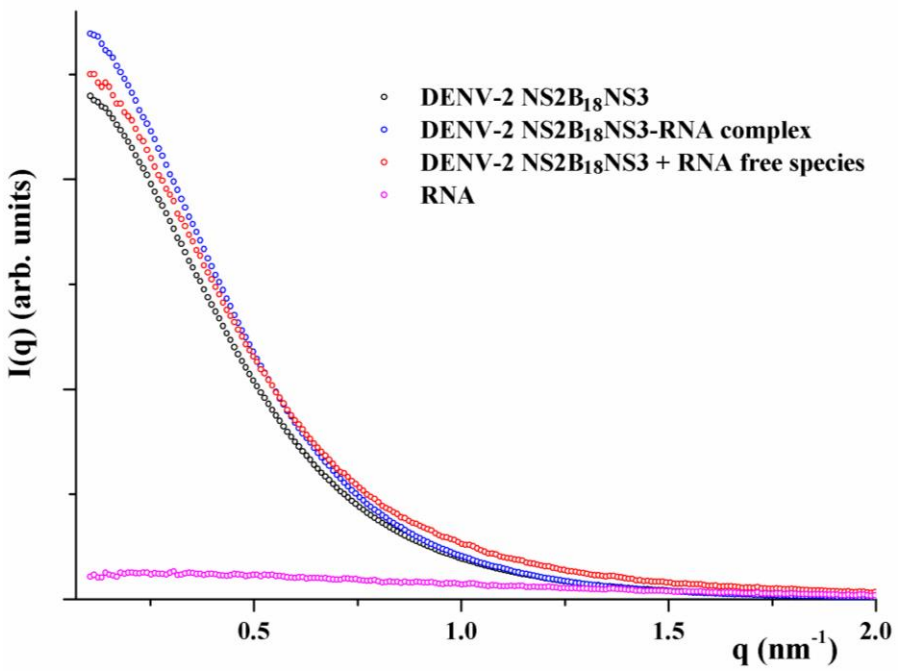

Supplementary Figure S9